

Image Augmentation Agent for Weakly Supervised Semantic Segmentation

Wangyu Wu^{1,2,3}, Xianglin Qiu¹, Siqu Song¹, Zhenhong Chen³,
Xiaowei Huang², Fei Ma^{1✉}, and Jimin Xiao^{1✉}

¹ Xi'an Jiaotong-Liverpool University
{Wangyu.Wu22,Xianglin.Qiu20,Siqu.Song22}@student.xjtlu.edu.cn
{fei.ma,jimin.xiao}@xjtlu.edu.cn
² The University of Liverpool
xiaowei.huang@liverpool.ac.uk
³ Microsoft
zcheh@microsoft.com

Abstract. Weakly-supervised semantic segmentation (WSSS) has achieved remarkable progress using only image-level labels. However, most existing WSSS methods focus on designing new network structures and loss functions to generate more accurate dense labels, overlooking the limitations imposed by fixed datasets, which can constrain performance improvements. We argue that more diverse trainable images provides WSSS richer information and help model understand more comprehensive semantic pattern. Therefore in this paper, we introduce a novel approach called *Image Augmentation Agent* (IAA) which shows that it is possible to enhance WSSS from data generation perspective. IAA mainly design an augmentation agent that leverages large language models (LLMs) and diffusion models to automatically generate additional images for WSSS. In practice, to address the instability in prompt generation by LLMs, we develop a prompt self-refinement mechanism. It allow LLMs to re-evaluate the rationality of generated prompts to produce more coherent prompts. Additionally, we insert an online filter into diffusion generation process to dynamically ensure the quality and balance of generated images. Experimental results show that our method significantly surpasses state-of-the-art WSSS approaches on the PASCAL VOC 2012 and MS COCO 2014 datasets.

Keywords: Weakly Supervised Learning · Semantic Segmentation · Diffusion Model · Large Language Model

1 Introduction

Weakly supervised semantic segmentation (WSSS) leverages image-level labels to achieve dense pixels segmentation. Current mainstream WSSS methods focus on designing new network architectures and loss functions to get better Class Activation Map (CAM) [24, 30, 35]. For example, MCTformer [31] designed a transformer with multi-class tokens to generate class-specific attention maps to

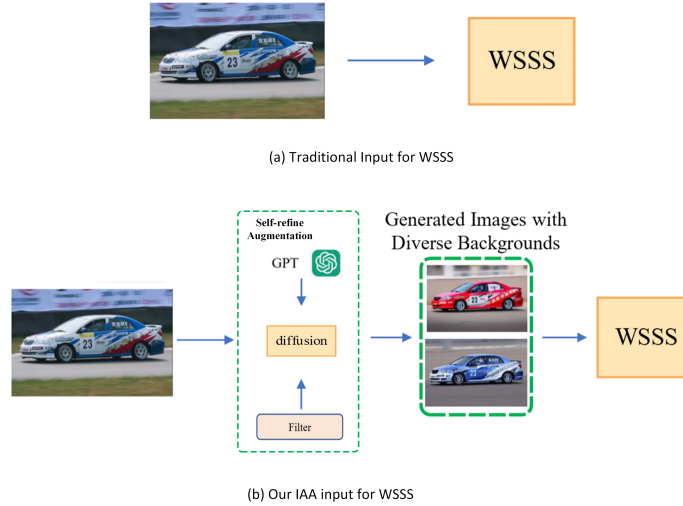


Fig. 1: (a) In the traditional WSSS framework, the original image is directly input into WSSS. (b) In our IAA, we utilize an augmentation agent to generate additional images and then combined with the original image and input into WSSS.

generate refine CAM. And the method presented in [24] incorporates a token contrastive loss for intra-class compactness and inter-class separability to mitigate over-smoothing CAM. However, these previous methods mentioned above are all only use limited scale of the available training data which restrict the performance improvement. Although previous work IACD [29] had explored using diffusion to generate augmented images for WSSS as shown in Fig. 1(b), the use of single background prompt resulted in insufficient image diversity, and the ex-post filtering operation for all generated data can easily lead to uneven number of the selected augmented images.

Building on the aforementioned problems, we propose a novel Image Augmentation Agent (IAA) to generate diverse and high-quality even synthetic training data for WSSS as shown in Fig. 1(b). Our main contributions can be summarized as follows:

- 1) We introduce a novel augmentation agent for WSSS, leveraging the capabilities of GPT and diffusion models to generate supplementary training images.
- 2) We present a self-refinement mechanism within the agent to ensure image quality, including the dynamic refinement of background prompts and the enhancement of generated images.
- 3) Our experimental results demonstrate that this framework significantly outperforms other state-of-the-art (SOTA) methods on the PASCAL VOC 2012 and MS COCO 2014 for the segmentation task.

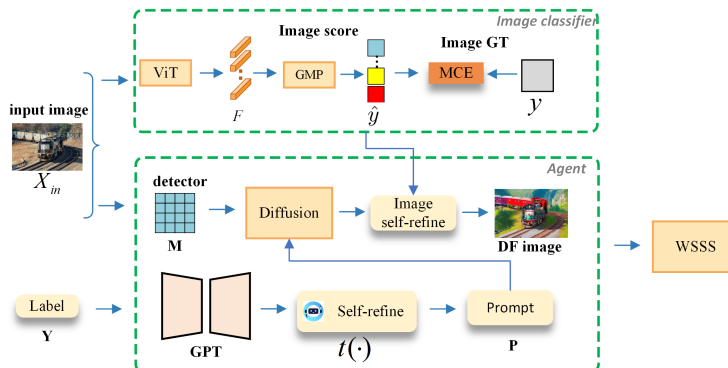


Fig. 2: Overall of our IAA. First, IAA uses image-level labels to generate text prompt through self-refine with GPT. Next, the original input image, self-refined GPT prompt and detector map are fed into the diffusion model to generate augmented images. Meanwhile, a pre-trained image classifier serves as a filter, performing image self-refinement to select high-quality images during diffusion generation process. Finally, the selected images are used for WSSS training.

2 Related Work

2.1 Weakly-Supervised Semantic Segmentation

Weakly Supervised Semantic Segmentation (WSSS) methods using image-level annotations commonly rely on Class Activation Maps (CAMs) as pseudo labels. However, CAMs often highlight only the most discriminative regions of objects, leaving less salient regions unutilized. Various approaches have been proposed to overcome this limitation, including region erasure [28], accumulating attention online [12], and mining cross-image semantics [27]. Techniques such as leveraging saliency maps [15] aim to reduce background interference and discover less obvious object regions. Additionally, contrastive methods [5] attempt to activate entire object regions by comparing pixel and prototype representations. Some studies, like [3], enhance WSSS by incorporating more category-specific information or leveraging additional learning signals from the training data. Recent advancements have explored integrating Vision Transformers (ViTs) into WSSS. For instance, MCTformer [31] utilizes ViT attention maps to create localization maps, while AFA [23] leverages multi-head self-attention and affinity modules for propagating pseudo labels. ViT-PCM [22] pioneers CAM-independent ViT applications for WSSS. These methods primarily optimize network structures or include additional features, often constrained by dataset size. In contrast, our work focuses on data augmentation, generating additional training data to advance WSSS.

2.2 Prompt-based Language Models

Prompt-based learning enhances pre-trained language models (PLMs) by appending task-specific instructions to inputs. Early strategies employed manually crafted prompts to tackle specific tasks [36]. However, manually designed prompts are inflexible and challenging to adapt to new tasks, prompting research into automatic prompt generation [25]. Continuous prompt optimization [17] has further advanced the field, improving adaptability and effectiveness across diverse tasks. Beyond text-based applications, PLMs have recently shown potential in vision tasks; for instance, [34] uses prompts to enhance few-shot learning. Distinctly, our approach employs PLMs to generate diverse prompts, enriching textual descriptions for WSSS. To the best of our knowledge, this is the first work that utilizes self-refinement PLMs to improve WSSS through diverse prompt generation.

2.3 Diffusion Probabilistic Model

Diffusion Probabilistic Models (DPMs), introduced by [26], have seen substantial progress in image generation. Latent Diffusion Models (LDMs) [20] refine this process by performing diffusion in latent spaces [7], significantly lowering computational requirements. Text-to-image diffusion models, leveraging CLIP [19] and similar pre-trained language models, have achieved remarkable image synthesis results by transforming text into latent representations. Enhanced by methods such as Stable Diffusion [21] and ControlNet [33], DPMs now generate high-quality images with precision and minimal artifacts. Recent studies [11] demonstrate the utility of DPMs in generating supplementary training data, thereby boosting task performance. Harnessing the strengths of DPMs, we propose IAA, which integrates conditional DPMs and GPT-generated prompts for WSSS. This represents the first application of conditional diffusion models in this context.

3 Methodology

In this section, we will outline the overall architecture and key components of our method. We start with an overview of our IAA in Sec.3.1, which integrates multiple agents with ControlNet diffusion and GPT, combined with self-refinement for generating additional images. Subsequently, in Sec.3.2, we present our proposed auto-refine Prompt method in the agent to generate diverse background prompts. Finally, in Sec. 3.3, we propose generating augmented data using diffusion with image self-refinement to produce high-quality images. The objective is to generate augmented images through our augmentation agent, increasing the training data size to ultimately enhance semantic segmentation performance.

3.1 Overall framework

As illustrated in Fig. 2, the components and process of our IAA framework are illustrated. We use ControlNet [33] as the diffusion [21] backbone and GPT-4o [1] as the LLM. We pre-train the image classifier as an image selector using

ViT with the original training data. The image class label is input into the LLM module, and we design a self-refinement process to improve prompt quality. The augmentation module uses the training image and the refined prompt from the LLM as input to generate the augmented image. We integrate the classifier as a filter into the diffusion step before generating the image to ensure that each augmented image is of high quality and control the class distribution of generate images. Finally, the training image combined with the augmented image is used as the final input for the WSSS task.

3.2 Prompt Generation with Self-Refinement

The motivation for generating prompts is to leverage LLM knowledge to create diverse background prompts that guide the diffusion model in generating images of different styles. Due to the instability of LLMs [18], we designed a self-refining prompt method for background prompt generation, as shown in Algorithm 1, which is the module $t(\cdot)$ in Fig. 2 . This method ensures that the generated background prompts are both reasonable and aligned with the current category through self-refinement within our agent.

Algorithm 1: Self-Refine for prompt generation

Input : category label Y , model GPT-4o, prompts $\{p_{gen}, p_{refine}\}$, quality threshold ϵ
Output: P

- 1 $y_0 = \text{GPT-4o}(\text{Initial_prompt}(p_{gen}, Y));$
- 2 **repeat**
- 3 $score_{y_0} = \text{GPT-4o}(\text{Refine_prompt}(p_{refine}, Y, y_0));$
- 4 $y_0 = \text{GPT-4o}(\text{Initial_prompt}(p_{gen}, Y));$
- 5 **until** $score_{y_0} < \epsilon;$
- 6 $P = y_0;$
- 7 **return** $P;$

In the WSSS setting, we denote training images as X_{in} and their corresponding labels as Y . As depicted in Fig. 2, for each of the N categories involved in the dataset, a pre-defined template P_{gen} is served as language commands for GPT-4o [1] to generate initial text output y_0 , which ensures the relevance and variety of language commands for generating background prompts.

$$y_0 = \text{GPT-4o}(\text{Initial_prompt}(p_{gen}, Y)), \quad (1)$$

Where p_{gen} , as shown in Fig.3(a), is the initial text prompt for generating synthetic samples of category Y , and it will be self-refined in our Algorithm 1. We use the refined prompt template p_{refine} in Fig.3b to assess the background prompt quality score. The output $score_{y_0}$, as shown in Fig.3(c), provides a score

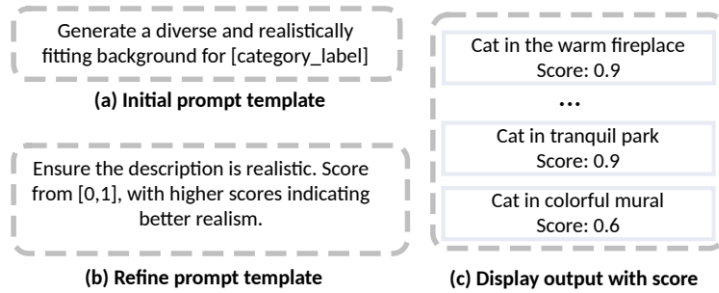


Fig. 3: (a) the manual template for LLM prompt generation; (b) the prompt template for prompt refinement; (c) the evaluation score of LLM output.

for the background. We then select the high-scoring prompt as our final output P , which will be used as the prompt in the diffusion models.

3.3 Diffusion with Image Self-Refinement

The motivation for using diffusion with image self-refinement is to leverage the ability of controlled diffusion to generate new images similar to the original ones, and to ensure image quality through our designed image self-refinement. By enriching the training data with additional enhanced images, we aim to improve the final performance of the WSSS task. To assess image quality, we trained a classifier using the original training data with image labels. As shown in Fig. 2, a ViT-based patch-driven classifier is first trained using the original dataset with image-level labels. To train the classifier, the input image X_{in} is divided into s input patches $X_{patch} \in \mathbb{R}^{d \times d \times 3}$ with a fixed size, where $s = \frac{hw}{d^2}$. The patch embeddings $F \in \mathbb{R}^{s \times e}$ are then obtained using a ViT encoder. Next, a weight matrix $W \in \mathbb{R}^{e \times |\mathcal{C}|}$ and a softmax function are applied to produce the prediction scores $Z \in \mathbb{R}^{s \times |\mathcal{C}|}$ for each patch:

$$Z = \text{softmax}(FW), \quad (2)$$

where \mathcal{C} is the set of categories in the dataset. Global maximum pooling (GMP) is then used to select the highest prediction scores $\hat{y} \in \mathbb{R}^{1 \times |\mathcal{C}|}$ in each class among all patches. Finally, \hat{y} is utilized as the prediction scores for the image-level classification and the classifier is trained via using the multi-label classification prediction error (MCE):

$$\begin{aligned} \mathcal{L}_{MCE} &= \frac{1}{|\mathcal{C}|} \sum_{c \in \mathcal{C}} BCE(y_c, \hat{y}_c) \\ &= -\frac{1}{|\mathcal{C}|} \sum_{c \in \mathcal{C}} y_c \log(\hat{y}_c) + (1 - y_c) \log(1 - \hat{y}_c), \end{aligned} \quad (3)$$

where, \hat{y}_c is the prediction score of class c and y_c is the ground-truth label. Once the classifier finishes the training, we can use it to select the high-quality generated training data.

Next, we integrate the pre-train classifier into the image self-refinement module. The classifier is incorporated into the diffusion generation step. If the augmented images do not meet the quality criteria, we continue generating images until the desired quality is achieved, rather than applying a filter after all images have been generated. This approach ensures that the augmented images are evenly distributed across all images, preventing the randomness of diffusion from causing some images to have more augmented versions than others. As shown in Fig. 2, in the diffusion module, we utilize Stable Diffusion with ControlNet [33] as our generative model. In the data augmentation stage, an input image $X_{in} \in \mathbb{R}^{h \times w \times 3}$, a text prompt P generated by the GPT self-refinement module, and a detection map M are feed into diffusion $\delta(\cdot)$ to generate a new training data X_{df} . The detection map is an extra condition (*e.g.*, Canny Edge [6] and Openpose [2]) to control the generation results.

$$X_{df} = \delta(X_{in}, M, P). \quad (4)$$

More details about the data augmentation process are described in Algorithm 2. For images belonging to the 'person' class, we utilize a pose detector map, while for images of other classes, we employ an edge detector map. Subsequently, we utilize GPT-prompt with the detector map to generate augmentation images.

Algorithm 2: Image Diffusion with Self-Refinement

Input: an input image X_{in} , an image-level label Y
Output: a generated image X_{aug}

- 1 $P \leftarrow \text{generate_prompt}(Y)$
- 2 **for** $t \in \{0, 1, \dots\}$ **do**
- 3 **if** "person" $\in Y$ **then**
- 4 $M \leftarrow \text{detect_map}(X_{in}, \text{human_pose})$
- 5 **else**
- 6 $M \leftarrow \text{detect_map}(X_{in}, \text{canny_edge})$
- 7 $X_{df} \leftarrow \delta(X_{in}, M, P)$
- 8 $\text{score}_{df} \leftarrow \text{classifier_score}(X_{df})$
- 9 **if** $\text{score}_{df} > \text{high_quality_threshold}$ **then**
- 10 **break**
- 11 $X_{aug} \leftarrow X_{df}$

3.4 Final Training Dataset of WSSS

After selecting the high-quality generated training samples, the synthetic dataset \mathcal{D}_{aug} and the original dataset \mathcal{D}_{origin} are combined as an extended dataset \mathcal{D}_{final} for the training of WSSS: $\mathcal{D}_{final} = \mathcal{D}_{origin} \cup \mathcal{D}_{aug}$.

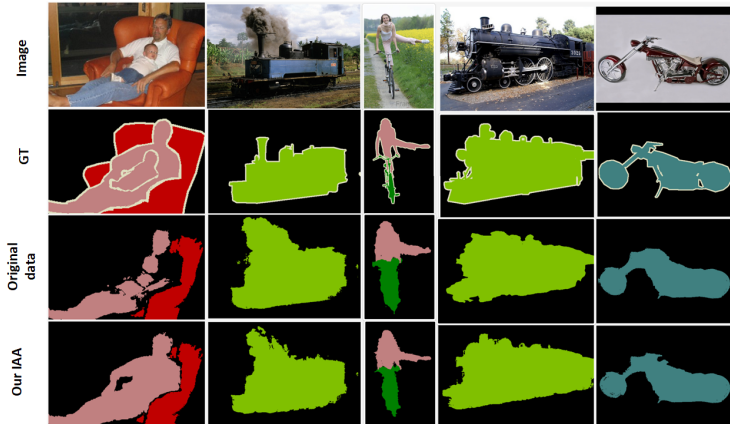


Fig. 4: Visualization of segmentation results on PASCAL VOC and MS COCO.

4 Experiments

In this section, we first present the details of the dataset, evaluation metrics, and implementation. Next, we compare our IAA with state-of-the-art methods on the PASCAL VOC 2012 and MS COCO 2014 benchmarks. Finally, we conduct ablation studies to demonstrate the effectiveness of the proposed method.

Dataset and Evaluated Metric. Our experiments are conducted on the PASCAL VOC 2012 dataset [8], which includes 21 categories, and MS COCO 2014 [16], featuring 81 classes. The PASCAL VOC 2012 dataset is commonly expanded using the SBD dataset [10]. For training on PASCAL VOC 2012, we use 10,582 images with image-level labels and 1,449 images for the validation set. In the case of the MS COCO 2014 dataset, approximately 82k images are used for training and around 40k images for validation, with the training images having only image-level annotations. The mean Intersection-over-Union (mIoU) is used as the evaluation metric.

Implementation Details. Our IAA integrates knowledge from pre-trained GPT-4o, Stable Diffusion [21], and ControlNet [33]. We utilize ViT-B/16 as the ViT model. To facilitate the training of the patch-based image classifier, images are resized to 384×384 as [14], and the 24×24 encoded patch features are preserved as input. The model is trained for up to 80 epochs with a batch size of 16, using $\epsilon = 0.9$ as the high-quality threshold for both text and image. Our final training dataset serves as input for the WSSS framework, while keeping all other settings consistent with ViT-PCM [22]. The experiments were conducted using two NVIDIA 4090 GPUs. Finally, we used the same verification tasks and settings as ViT-PCM [22].

4.1 Final Segmentation Performance

Comparison with State-of-the-arts. To evaluate our approach, we train fully supervised models using the pseudo labels from our generated images and compare the segmentation performance with other SOTA methods. As shown in

Table 1: Semantic Segmentation Performance Comparison (mIoU) on MS COCO 2014 and PASCAL VOC 2012.

Model	Pub.	Backbone	VOC	COCO
TSCD [32]	AAAI23	MiT-B1	67.3	40.1
SAS [13]	AAAI23	ViT-B/16	69.5	44.5
FPR [4]	ICCV23	ResNet38	70.0	43.9
ToCo [24]	CVPR23	ViT-B	70.2	42.3
SFC [35]	AAAI24	ViT-B/16	71.2	44.6
IACD [29]	ICASSP24	ViT-B/16	71.4	44.3
PGSD [9]	TCSVT24	ViT-B/16	68.7	43.9
IAA	Ours	ViT-B/16	72.3	45.3



Fig. 5: Visualizations of ControlNet Generated Images include original training data and augmented images.

Tab. 1, our method outperforms existing SOTA approaches in final segmentation performance.

Visualization of results. Our IAA effectively leverages an augmentation agent, integrating GPT-4o and diffusion knowledge, to enrich the training data for WSSS. Fig. 5 presents the augmented data used as additional training input. Furthermore, Fig. 4 showcases visualization examples of segmentation outputs. It can be observed that our method consistently achieves more precise segmentation results.

4.2 Ablation Studies

We conduct ablation studies to assess the impact of our two key contributions: prompt self-refinement and image self-refinement. As shown in Table 2, we integrated the diffusion augmentation method into the original train (no augmentation data) without any self-refinement, resulting in a 0.2% decrease in mIoU

Table 2: Ablation studies on main components of the proposed framework. DA: Diffusion Augmentation; ISR: Image Self-Refinement; PSR: Prompt Self-Refinement on the Pascal VOC 2012 val.

Original Train	DA	ISR	PSR	mIoU
✓				69.3%
✓	✓			69.1%
✓	✓	✓		71.7%
✓	✓	✓	✓	72.3%

on the validation set. We speculate that this decline is due to the randomness of the diffusion process, which may have introduced low-quality augmented images. After incorporating image self-refinement during the generation phase of diffusion model, the performance improved by 2.4%, shows that our approach effectively enhances image quality. Finally, we introduced prompt self-refinement to diversify the background of the diffusion images, which further increased performance by 0.6%. It proves the importance of diverse and reliable prompts for image generation.

5 Conclusion

In this work, we propose an IAA method for WSSS. Unlike previous approaches that solely rely on the original training data, we employ an augmentation agent combined with diffusion and LLM knowledge to generate additional training images. These generated images are then combined with the original training data to create the final dataset, increasing the overall training data size. Furthermore, we design a self-refinement prompt and a self-refinement image module to enhance image quality. Ultimately, our data augmentation method achieves SOTA results in WSSS.

ACKNOWLEDGMENT

This work was supported by the National Natural Science Foundation of China (No. 62471405, 62331003, 62301451), Suzhou Basic Research Program (SYG202316) and XJTLU REF-22-01-010, XJTLU AI University Research Centre, Jiangsu Province Engineering Research Centre of Data Science and Cognitive Computation at XJTLU and SIP AI innovation platform (YZCXPT2022103).

References

1. Bubeck, S., Chandrasekaran, V., Eldan, R., Gehrke, J., Horvitz, E., Kamar, E., Lee, P., Lee, Y.T., Li, Y., Lundberg, S., et al.: Sparks of artificial general intelligence: Early experiments with gpt-4. arXiv preprint arXiv:2303.12712 (2023)

2. Cao, Z., Simon, T., Wei, S.E., Sheikh, Y.: Realtime multi-person 2d pose estimation using part affinity fields. In: Proc. IEEE Conf. Comput. Vis. Pattern Recog. pp. 7291–7299 (2017)
3. Chang, Y.T., Wang, Q., Hung, W.C., Piramuthu, R., Tsai, Y.H., Yang, M.H.: Weakly-supervised semantic segmentation via sub-category exploration. In: Proc. IEEE Conf. Comput. Vis. Pattern Recog. pp. 8991–9000 (2020)
4. Chen, L., Lei, C., Li, R., Li, S., Zhang, Z., Zhang, L.: Fpr: False positive rectification for weakly supervised semantic segmentation. In: Proc. IEEE Int. Conf. Comput. Vis. pp. 1108–1118 (2023)
5. Chen, Q., Yang, L., Lai, J.H., Xie, X.: Self-supervised image-specific prototype exploration for weakly supervised semantic segmentation. In: Proc. IEEE Conf. Comput. Vis. Pattern Recog. pp. 4288–4298 (2022)
6. Ding, L., Goshtasby, A.: On the canny edge detector. *Pattern recognition* **34**(3), 721–725 (2001)
7. Esser, P., Rombach, R., Ommer, B.: Taming transformers for high-resolution image synthesis. In: Proc. IEEE Conf. Comput. Vis. Pattern Recog. (2021)
8. Everingham, M., Van Gool, L., Williams, C.K., Winn, J., Zisserman, A.: The pascal visual object classes (VOC) challenge. *Int. J. Comput. Vis.* **88**, 303–338 (2010)
9. Hao, X., Jiang, X., Ni, W., Tan, W., Yan, B.: Prompt-guided semantic-aware distillation for weakly supervised incremental semantic segmentation. *IEEE Transactions on Circuits and Systems for Video Technology* (2024)
10. Hariharan, B., Arbeláez, P., Bourdev, L., Maji, S., Malik, J.: Semantic contours from inverse detectors. In: Proc. IEEE Int. Conf. Comput. Vis. pp. 991–998 (2011)
11. Ho, J., Jain, A., Abbeel, P.: Denoising diffusion probabilistic models. *Advances in Neural Information Processing Systems* **33**, 6840–6851 (2020)
12. Jiang, P.T., Hou, Q.: Integral object mining via online attention accumulation. In: Proc. IEEE Int. Conf. Comput. Vis. pp. 2070–2079 (2019)
13. Kim, S., Park, D., Shim, B.: Semantic-aware superpixel for weakly supervised semantic segmentation. In: AAAI Conf. Artif. Intell. vol. 37, pp. 1142–1150 (2023)
14. Kolesnikov, A., Lampert, C.H.: Seed, expand and constrain: Three principles for weakly-supervised image segmentation. In: Eur. Conf. Comput. Vis. pp. 695–711 (2016)
15. Lee, S., Lee, M., Lee, J., Shim, H.: Railroad is not a train: Saliency as pseudo-pixel supervision for weakly supervised semantic segmentation. In: Proc. IEEE Conf. Comput. Vis. Pattern Recog. pp. 5495–5505 (2021)
16. Lin, T.Y., Maire, M., Belongie, S., Hays, J., Perona, P., Ramanan, D., Dollár, P., Zitnick, C.L.: Microsoft coco: Common objects in context. In: Eur. Conf. Comput. Vis. pp. 740–755. Springer (2014)
17. Liu, X., Zheng, Y., Du, Z., Ding, M., Qian, Y., Yang, Z., Tang, J.: Gpt understands, too. *AI Open* (2023)
18. Madaan, A., Tandon, N., Gupta, P., Hallinan, S., Gao, L., Wiegrefe, S., Alon, U., Dziri, N., Prabhunoye, S., Yang, Y., et al.: Self-refine: Iterative refinement with self-feedback. *Int. Conf. Neur. Info. Process. Sys.* **36** (2024)
19. Radford, A., Kim, J.W., Hallacy, C., Ramesh, A., Goh, G., Agarwal, S., Sastry, G., Askell, A., Mishkin, P., Clark, J., et al.: Learning transferable visual models from natural language supervision. In: International conference on machine learning. pp. 8748–8763. PMLR (2021)
20. Richardson, E., Alaluf, Y., Patashnik, O., Nitzan, Y., Azar, Y., Shapiro, S., Cohen-Or, D.: Encoding in style: a stylegan encoder for image-to-image translation. In: Proc. IEEE Conf. Comput. Vis. Pattern Recog. pp. 2287–2296 (2021)

21. Rombach, R., Blattmann, A., Lorenz, D., Esser, P., Ommer, B.: High-resolution image synthesis with latent diffusion models. In: Proc. IEEE Conf. Comput. Vis. Pattern Recog. pp. 10684–10695 (2022)
22. Rossetti, S., Zappia, D., Sanzari, M., Schaerf, M., Pirri, F.: Max pooling with vision transformers reconciles class and shape in weakly supervised semantic segmentation. In: Eur. Conf. Comput. Vis. pp. 446–463 (2022)
23. Ru, L., Zhan, Y., Yu, B., Du, B.: Learning affinity from attention: End-to-end weakly-supervised semantic segmentation with transformers. In: Proc. IEEE Conf. Comput. Vis. Pattern Recog. pp. 16846–16855 (2022)
24. Ru, L., Zheng, H., Zhan, Y., Du, B.: Token contrast for weakly-supervised semantic segmentation. In: Proc. IEEE Conf. Comput. Vis. Pattern Recog. (2023)
25. Shin, T., Razeghi, Y., Logan IV, R.L., Wallace, E., Singh, S.: Autoprompt: Eliciting knowledge from language models with automatically generated prompts. arXiv preprint arXiv:2010.15980 (2020)
26. Sohl-Dickstein, J., Weiss, E., Maheswaranathan, N., Ganguli, S.: Deep unsupervised learning using nonequilibrium thermodynamics. In: Int. Conf. Mach. Learn. pp. 2256–2265 (2015)
27. Sun, G., Wang, W., Dai, J., Van Gool, L.: Mining cross-image semantics for weakly supervised semantic segmentation. In: Eur. Conf. Comput. Vis. (2020)
28. Wei, Y., Feng, J., Liang, X., Cheng, M.M., Zhao, Y., Yan, S.: Object region mining with adversarial erasing: A simple classification to semantic segmentation approach. In: Proc. IEEE Conf. Comput. Vis. Pattern Recog. pp. 1568–1576 (2017)
29. Wu, W., Dai, T., Huang, X., Ma, F., Xiao, J.: Image augmentation with controlled diffusion for weakly-supervised semantic segmentation. In: IEEE Int. Conf. Acoust. Speech Signal Process. pp. 6175–6179. IEEE (2024)
30. Wu, W., Dai, T., Huang, X., Ma, F., Xiao, J.: Top-k pooling with patch contrastive learning for weakly-supervised semantic segmentation. IEEE SMC (2024)
31. Xu, L., Ouyang, W., Bennamoun, M., Boussaid, F., Xu, D.: Multi-class token transformer for weakly supervised semantic segmentation. In: Proc. IEEE Conf. Comput. Vis. Pattern Recog. pp. 4310–4319 (2022)
32. Xu, R., Wang, C., Sun, J., Xu, S., Meng, W., Zhang, X.: Self correspondence distillation for end-to-end weakly-supervised semantic segmentation. In: AAAI Conf. Artif. Intell. vol. 37, pp. 3045–3053 (2023)
33. Zhang, L., Agrawala, M.: Adding conditional control to text-to-image diffusion models. arXiv preprint arXiv:2302.05543 (2023)
34. Zhang, R., Hu, X., Li, B., Huang, S., Deng, H., Qiao, Y., Gao, P., Li, H.: Prompt, generate, then cache: Cascade of foundation models makes strong few-shot learners. In: Proc. IEEE Conf. Comput. Vis. Pattern Recog. pp. 15211–15222 (2023)
35. Zhao, X., Tang, F., Wang, X., Xiao, J.: Sfc: Shared feature calibration in weakly supervised semantic segmentation. In: Proceedings of the AAAI Conference on Artificial Intelligence. vol. 38, pp. 7525–7533 (2024)
36. Zou, X., Yin, D., Zhong, Q., Yang, H., Yang, Z., Tang, J.: Controllable generation from pre-trained language models via inverse prompting. In: Proceedings of the 27th ACM SIGKDD Conference on Knowledge Discovery & Data Mining. pp. 2450–2460 (2021)